CRYSTAL GROWTH & DESIGN

pubs.acs.org/crystal

Article

Solvent and Guest-Driven Supramolecular Organic Frameworks Based on a Calix[4]arene-tetrol: Channels vs Molecular Cavities

Neal Hickey, Veronica Iuliano, Carmen Talotta, Margherita De Rosa, Annunziata Soriente, Carmine Gaeta, Placido Neri,* and Silvano Geremia*

Cite This: *Cryst. Growth Des.* 2021, 21, 6357−6363

Read Online

ACCESS | Metrics & More | Article Recommendations | Supporting Information

ABSTRACT: Cone-shaped calix[4]arene-tetrol **3** has the ability to form open structures due to the presence of four OH groups at the upper rim, which allows the construction of H-bonded supramolecular organic frameworks (SOFs). In the presence of water, SOF-1 is formed, which contains hydrophilic channels (mean diameter of 8.5 Å) contoured by the *p*-phenolic OH groups. In the presence of acetonitrile, SOF-2 is formed, which contains smaller hydrophobic channels (mean diameter of 6.6 Å) delimited by aromatic walls. The Na^+@**3** complex, which hosts acetonitrile molecules in the calixarene cavities, and dibromo-calix[4]arene-diol **5** give rise to more compact SOFs not containing channels. The H-bond network formed by all four *p*-phenolic OH groups in a pinched cone conformation of the calixarene is a determinant for the porosity of SOFs based on calix[4]arene-tetrol.

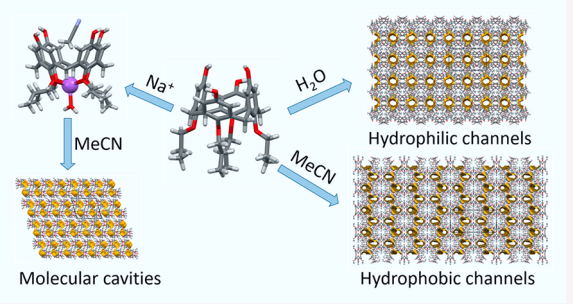

INTRODUCTION

Supramolecular organic frameworks (SOFs)[1−8] have attracted significant attention due to their potential applications in gas storage and separation.[9,10] SOFs are structural analogues of the well-known metal−organic frameworks (MOFs)[11−14] and covalent organic frameworks (COFs),[15,16] and can be defined as porous molecular solids built from organic subunits assembled through weak noncovalent interactions. The most common strategy for the construction of SOFs is based on the crystallization of its organic constituents from an appropriate solvent system, driven by supramolecular interactions such as hydrogen bond, halogen bond, $\pi-\pi$ stacking, and van der Waals interactions.[17−20] Because the framework interactions of SOFs are weaker and less directional in nature with respect to both MOFs and COFs, predictable and controlled assembly into well-defined systems can be more challenging.[21,22]

In recent years, macrocycle-based SOFs (M-SOFs) have emerged as an interesting class of crystalline porous materials because of the intrinsic molecular porosity of the constitutive macrocyclic building blocks, commonly based on calixarene,[23] bisurea,[24] cucurbituril,[25] and pillarene[26−28] skeletons. The peculiar structural features of the macrocyclic subunits, namely, their cyclic shape (often with an intrinsic pore) in conjunction with the easy introduction of multiple functional groups, provide a great variety of possible SOF architectures.[29] The increased rigidity of some specific macrocycles can often be useful for the spontaneous self-assembly of a porous network; however, the controlled packing of these macrocyclic subunits in the crystalline state remains of fundamental importance. In fact, the assembly of porous macrocycles does not always produce open crystal structures with channels, due to unfavorable crystal packing.

After the pioneering work of Atwood and co-workers, calixarene-based frameworks have become the most studied M-SOFs.[30] Among them, of prime importance are those driven by strong and directional H-bonding interactions. In this way, several beautiful examples of SOFs containing cavity or channels have been obtained by exploiting OH groups as supramolecular stitching points. Two interesting H-bonded SOFs were obtained from calix[4]arene-tetrahydroquinone **1**[31−33] and proximal calix[4]arene-dihydroquinone **2** (Figure 1),[34−38] whose nanochannels were used for the synthesis of silver nanowires and for CO_2 capture, respectively. Against this background, we have now studied cavity-shaped calix[4]arene-tetrol **3** (Figure 1),[39] bearing four OH groups at the upper rim for the construction of a H-bonded framework and four OPr groups at the lower rim to maintain its cone conformation. The effects on the crystal engineering of various solvents with different polarity and guest properties were investigated. Furthermore, the influence of a sodium guest, which makes

Received: July 22, 2021
Revised: October 4, 2021
Published: October 15, 2021

https://doi.org/10.1021/acs.cgd.1c00828
Cryst. Growth Des. 2021, 21, 6357−6363

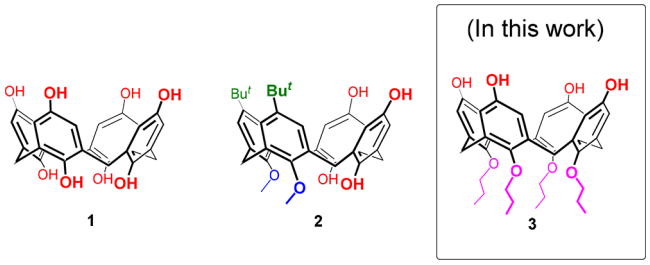

Figure 1. Chemical drawing of calix[4]arene-tetrahydroquinone **1**, proximal calix[4]arene-dihydroquinone **2**, and calix[4]arene-tetrol **3**.

the cone conformation more rigid and symmetric, was also investigated.

EXPERIMENTAL SECTION

General Information. Anhydrous reactions were conducted under inert atmosphere (nitrogen) using dry solvents. The commercial reagents were purchased from Merck and TCI chemicals and were used without further purification. The reactions were controlled by thin-layer chromatography (TLC) with Merck plates coated with silica gel (0.25 mm) and fluorescence indicator UV_{254} and visualized using UV light and nebulization with an indicator solution of H_2SO_4−$Ce(SO_4)_2$. The reaction products were purified by Macherey-Nagel silica gel chromatography (60, 70-230 mesh). The melting point was determined using a STUART SMP30 instrument. NMR spectra were recorded on a Bruker Avance-600 spectrometer [600 (^{1}H) and 150 MHz (^{13}C)] and Bruker Avance-400 spectrometer [400 (^{1}H) and 100 MHz (^{13}C)]. Chemical shifts are reported relative to the residual solvent peak ($CHCl_3$: δ 7.26, $CDCl_3$: δ 77.16; CH_3OH: δ 3.31, CD_3OD: δ 49.00).[40] HR MALDI mass spectra were recorded on a Bruker Solarix FT-ICR mass spectrometer equipped with a 7T magnet. The samples recorded in MALDI were prepared by mixing 10 μL of analyte in chloroform or methanol (1 mg/mL) with 10 μL of solution of 2,5-dihydroxybenzoic acid (10 mg/mL in methanol). The mass spectra were calibrated externally, and a linear calibration was applied. Thermal analyses were performed using a TGA 2 instrument (Mettler Toledo).

Synthesis of Derivative 5. To a solution of tetrabromo derivative **4** (0.20 g, 0.20 mmol) in freshly distilled THF (34 mL), *n*-BuLi (7.0 mL of 2.5 M solution in hexane, 18.0 mmol) was added at −78 °C, and the mixture was stirred at this temperature for 75 min. Trimethyl borate (3.0 mL, 31.0 mmol) was then added at −78 °C, and the mixture was allowed to warm to room temperature. After 5 h, the reaction mixture was cooled again to −78 °C, and H_2O_2 (3.3 mL of 30% aq solution) and NaOH (8.0 mL of 3 N aq solution) were added. The resulting solution was stirred overnight at room temperature, after which the solution was concentrated in vacuo and subsequently diluted with DCM (100 mL). The mixture was washed with H_2O (2 × 50 mL). The combined organic phases were dried over anhydrous Na_2SO_4, filtered, and concentrated in vacuo. The raw product was purified through a silica gel chromatography column using solvent mixture 70:30 petroleum ether/chloroform as eluent. Derivative **5** was isolated with 73% yield (0.13 g, 0.2 mmol). Mp: >260 °C dec. ^{1}H NMR ($CDCl_3$, 400 MHz, 298 K): δ 7.16 (s, Ar*H*, 4H), 5.71 (s, Ar*H*, 4H), 4.36 and 3.05 (AX system, J = 13.5, ArCH_2Ar, 8H), 3.92 (t, J = 6.7 Hz, −O$CH_2$$CH_2$$CH_3$, 4H), 3.63 (t, J = 6.4 Hz, −O$CH_2$$CH_2$$CH_3$, 4H), 1.84 (overlapped, −O$CH_2$$CH_2$$CH_3$, 8H), 1.06 (t, J = 6.8 Hz, −O$CH_2$$CH_2$$CH_3$, 6H), 0.87 (t, J = 6.7 Hz, −O$CH_2$$CH_2$$CH_3$, 6H); ^{13}C{^{1}H} NMR ($CDCl_3$, 100 MHz, 298 K): δ 157.2, 150.2, 150.1, 138.8, 134.2, 131.5, 115.3, 114.5, 77.1, 76.8, 31.1, 23.5, 23.1, 10.9, 10.0. MALDI-MS: m/z $[M]^+$ calcd for $C_{40}H_{46}Br_2O_6^+$ 782.1641; found 782.1677; $[M + Na]^+$ calcd for $C_{40}H_{46}Br_2NaO_6^+$ 805.1533; found 805.1592.

Synthesis of Derivative 3. To a solution of derivative **5** (0.08 g, 0.10 mmol) in freshly distilled THF (15 mL), *n*-BuLi (3.0 mL of 2.5 M solution in hexane, 7.5 mmol) was added at −78 °C, and the mixture was stirred at this temperature for 75 min. Trimethyl borate (2.0 mL, 15.5 mmol) was then added at −78 °C, and the mixture was allowed to warm to room temperature. After 5 h, the reaction mixture was cooled again to −78 °C, and H_2O_2 (2 mL of 30% aq solution) and NaOH (4 mL of 3 N aq solution) were added. The resulting solution was stirred overnight at room temperature, after which the solution was concentrated in vacuo and subsequently diluted with ethyl acetate (50 mL). The mixture was washed with H_2O (2 × 25 mL). The combined organic phases were dried over anhydrous Na_2SO_4, filtered, and concentrated in vacuo. The crude product was purified through a silica gel chromatography column using solvent mixture 90:10 chloroform/methanol as eluent. Derivative **3** was isolated with 43% yield (0.029 mg, 0.04 mmol). Mp: >320 °C dec. ^{1}H NMR (CD_3OD, 600 MHz, 298 K): δ 6.17 (s, Ar*H*, 8H), 4.36 and 2.94 (AX system, J = 13.1, ArCH_2Ar, 8H), 3.76 (t, J = 7.4 Hz, −O$CH_2$$CH_2$$CH_3$, 8H), 1.94 (m, −O$CH_2$$CH_2$$CH_3$, 8H), 1.01 (t, J = 7.5 Hz, −O$CH_2$$CH_2$$CH_3$, 12H). MALDI-MS: m/z $[M]^+$ calcd for $C_{40}H_{48}O_8^+$ 656.3349; found 656.3336; $[M + Na]^+$ calcd for $C_{40}H_{48}NaO_8^+$ 679.3241; found 679.3233; $[M+K]^+$ calcd for $C_{40}H_{48}KO_8^+$ 695.2981; found 695.2974.

Crystallization. SOF-1: 4.1 mg of compound **3** was dissolved in 1.3 mL of a 9:1 chloroform/methanol hot mixture and crystallized by slow evaporation, obtaining single crystals suitable for X-ray diffraction. SOF-2: 4.0 mg of compound **3** was dissolved in 1.3 mL of a 9:1 chloroform/acetonitrile hot mixture and crystallized by slow evaporation obtaining single crystals suitable for X-ray diffraction. SOF-3: A mixture 1:1 of compound **3** (6.8 mg) and NaI (1.6 mg) was dissolved in 0.6 mL of a 3:1 chloroform/acetonitrile hot mixture and crystallized by slow evaporation obtaining single crystals suitable for X-ray diffraction. SOF-4: 5.5 mg of compound **5** was dissolved in 1 mL of hot methanol and crystallized by slow evaporation obtaining single crystals suitable for X-ray diffraction.

Single Crystal X-ray Diffraction. X-ray diffraction data collection was performed at the XRD1 beamline of the Elettra synchrotron (Trieste, Italy), employing the rotating-crystal method with a Dectris Pilatus 2 M area detector. In all cases, single crystals were dipped in paratone cryoprotectant, mounted on a nylon loop, and flash-frozen under a nitrogen stream at a 100 K. Details of data reduction and structure refinements are reported in the Supporting Information (SI). Additional X-ray diffraction experiments were performed on SOF-1 after treatment in air at room temperature and at 60 °C using a conventional source (see the SI).

RESULTS AND DISCUSSION

For the synthesis of cone-shaped calix[4]arene-tetrol **3**, we decided to apply a boronation strategy already described in the literature for tetrabromo-calix[4]arenes blocked in a 1,3-alternate conformation[41,42] but never reported for cone-shaped analogues.[43]

Starting from the known tetrabromo-calix[4]arene **4**,[44] a hydroboration/oxidation reaction was performed, which consists of three steps: (1) lithiation using *n*BuLi; (2) boron exchange with $B(OMe)_3$; (3) oxidation by H_2O_2/NaOH. Surprisingly, the application of this synthetic strategy only gave 1,3-dibromo-calix[4]arene-diol **5** in high yield (73%, Scheme 1), as confirmed by 1D NMR and FT ICR HR mass spectrometry (Figures S1−S5). Dibromocalix[4]arene **5** was further reacted under the above conditions to give calix[4]-arene-tetrol **3** in 43% yield. The structure of **3** was confirmed by 1D NMR and FT ICR HR mass spectrometry (Figures S6 and S7).

Crystallization of tetrol **3** in $CHCl_3$/CH_3OH solvent mixture provided solid-state assembly **SOF-1**, which was characterized by diffraction studies using synchrotron radiation at 100 K. The asymmetric unit of the monoclinic ($P2_1/c$) crystal is composed by three crystallographically independent molecules of tetrol **3**, 2.7 methanol (statistically distributed in

https://doi.org/10.1021/acs.cgd.1c00828
Cryst. Growth Des. 2021, 21, 6357−6363

Scheme 1. Synthesis of Calix[4]arene-tetrol 3

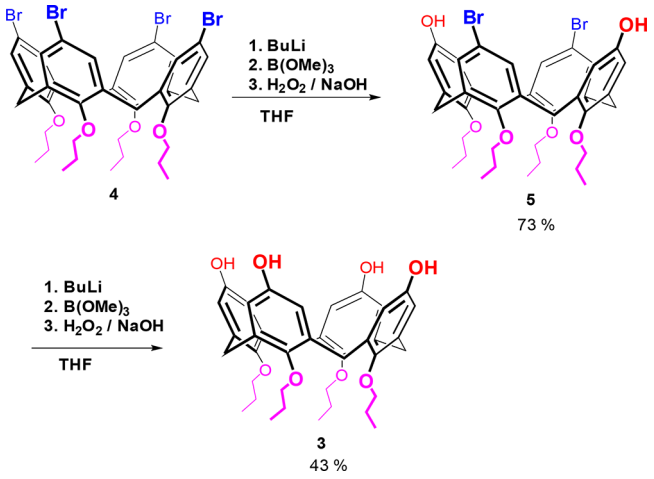

5 sites), and 8.4 water (statistically distributed in 18 sites) molecules (Figure S8). The macrocycles show the expected cone conformation (Figure 2a,b).

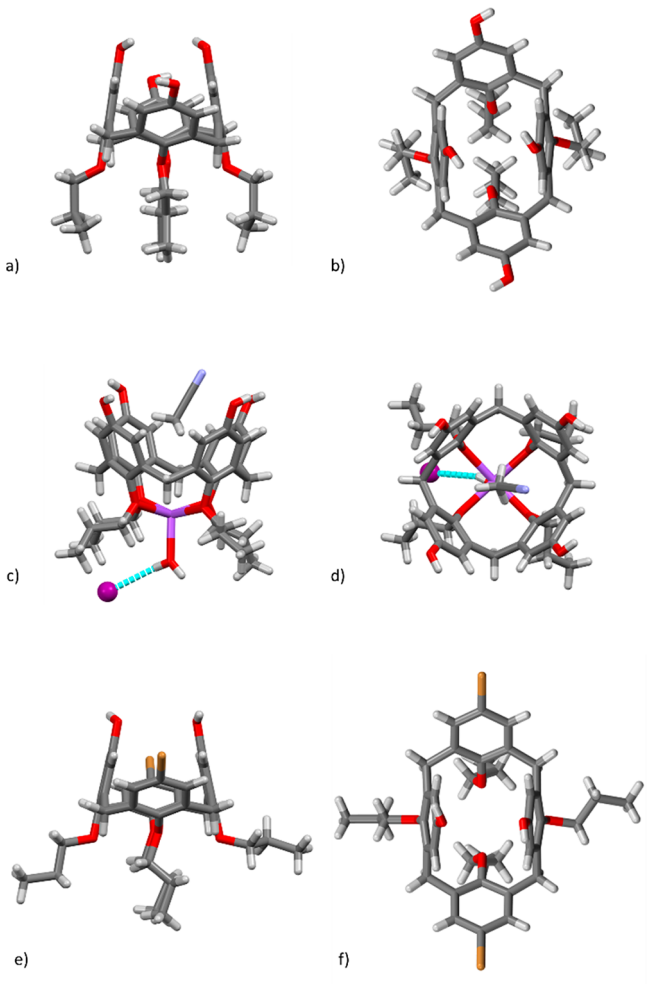

Figure 2. Stick representation of molecular structures obtained by X-ray diffraction. Side and top views of one calix[4]arene-tetrol **3** molecule (a, b); Na^+@**3** complex (c, d), and dibromocalix[4]arene-diol **5** (e, f). The atomic species are represented in CPK colors.

In particular, all three crystallographically independent molecules show a pseudo C_{2v} symmetry with two opposite phenyl rings more outwardly inclined (range 131−144°) with the other two nearly orthogonal (range 80−86°) with respect to the corresponding mean plane of the methylene bridging groups. Angles smaller (or larger) than 90° indicate that the hydroxy groups on the upper rims are inward (or outward) oriented with respect to the center of the cone. The solid-state molecules are less symmetric with respect to the C_{4v} symmetry of **3** observed in solution. This can be attributed to a fast (relative to the NMR time scale) conformational interconversion in solution between two pinched cone structures (known as "breathing of the calixarene").[45] The pinched cone conformation dramatically restricts the access to the calixarene cavity, with the short O···O phenolic distance ranging from 3.86 to 4.56 Å across the three independent molecules. On the contrary, this conformation permits the formation of an extended network of intermolecular hydrogen bond chains involving the *p*-hydroxy functions of **3**. This generates nanochannels (Figure 3a−c) delimited by repeated units of

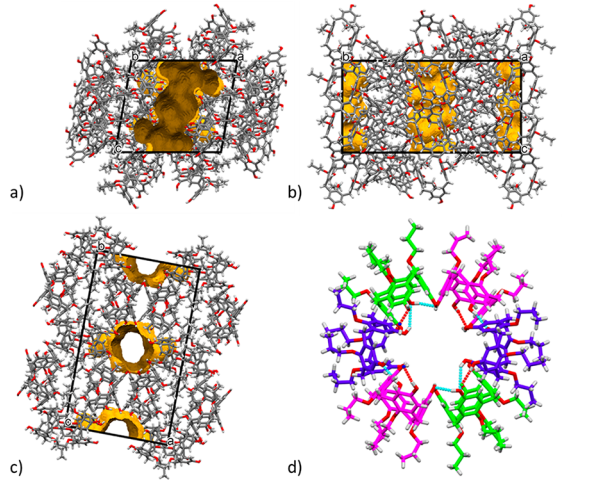

Figure 3. Supramolecular structure of SOF-1. Orthogonal representation of the crystal packing (a−c) following the convention used in the International Tables of Crystallography. Stick models of **3** in CPK colors and contact surface contours defining the nanochannels in the unit cell are shown. (d) Nanochannels generated by a repeated hexameric ring formed by three independent molecules of **3** (blue, green and magenta) with their centrosymmetric equivalents, as viewed along the *c* axis.

the three independent molecules with their centrosymmetric equivalents, thereby forming a hexameric ring (Figure 3d). These interconnected H-bonded molecules are all oriented with the calixarene cups toward the center of the channel. The hexamers, translationally repeated along the *c* axis of the crystal, are also interconnected by H-bonds. In this porous open structure, these channels correspond to 16.3% of the total crystal volume. The mean diameter of each channel is about 8.5 Å with a minimum diameter of 5.2 Å. These highly polar channels are partially filled with the above-mentioned disordered H_2O/CH_3OH solvent molecules, which form a dense H-bond network between the solvent molecules and the *p*-hydroxy functions of molecules **3** (Figure S9a). Thermogravimetric analysis (TGA) indicates that these solvent molecules can be completely removed below 100 °C (Figure S16).

https://doi.org/10.1021/acs.cgd.1c00828
Cryst. Growth Des. 2021, 21, 6357−6363

Attempts to remove the solvent molecules of SOF-1, while maintaining the crystallinity of the sample, indicated that the crystals are stable in air for several days maintaining the coordinated water molecules (Figure S18). After thermal treatment at 60 °C, while the crystal habit and unit cell remain substantially unchanged (Table S2), the diffraction pattern significantly deteriorates (Figure S19).

The parallel nanochannels are arranged in a rectangular lattice of 17.2 × 20.1 Å^2 (Figure S10). The interchannel space, which does not contain solvent molecules, is efficiently filled by the lipophilic lower rim propyl chains arranged in various conformations that maximize the van der Waals interactions. Crystallization of tetrol **3** in $CHCl_3/CH_3CN$ solvent provides the solid-state assembly SOF-2, which was also characterized by diffraction studies using synchrotron radiation. The asymmetric unit of the monoclinic ($C2/c$) crystal is composed of one and a half crystallographically independent molecules of tetrol **3** and three CH_3CN cocrystallized solvent molecules (Figure S11). The conformations of the tetrol **3** molecules are similar to those observed for SOF-1, with a pseudo C_{2v} or exactly C_2 symmetry for those molecules which lie on crystallographic 2-fold axes (Figure 2a,b). The dihedral angles of the more outwardly inclined phenyl rings range from 138 to 143°, while the dihedral angles of the nearly parallel phenyl rings range from 80 to 82° with respect to the methylene plane. The short O···O phenolic distances are 3.89 and 3.99 Å for the symmetric and pseudosymmetric molecules, respectively. This closed conformation does not permit the host−guest complexation of the solvent molecules, which are however found to be cocrystallized in channels created by the crystal packing (Figure S9b).

The most relevant supramolecular feature of SOF-2 is the presence of two distinct linear polymeric chain assemblies of **3** propagating by H-bonding interactions involving the calixarene OH groups (Figure 4). In one, each molecule with crystallographic 2-fold symmetry stitches to two other equivalent molecules. The intermolecular interaction is characterized by four symmetric strong H-bonds involving the hydroxyls of the two pinched phenyl rings of one molecule with one of the two outward oriented phenyl group of another molecule, and vice versa (Figure 4a). The space group operators generate, for this symmetric molecule, a cyclic network of synergic H-bonds involving four OH groups of three equivalent molecules (Figure 4b). A similar polymeric chain is observed for the other crystallographically independent molecule. However, in this case, the cyclic network of H-bonds is interrupted by the insertion of the acetonitrile molecule (Figure 4c), which forms a strong H-bond and deforms the chain by breaking its 2-fold symmetry (Figure 4d). The crystal packing of these parallel polymeric chains, which run along the c axis, is characterized by the presence of nanochannels delimited by three chains (Figure 5), one symmetric (blue in Figure 5d) and two nonsymmetric (green in Figure 5d), which are partially filled by the cocrystallized acetonitrile molecules (Figure S9b). TGA indicated that this solvent can be removed at low temperature (Figure S17). The channels walls are mainly formed by the pinched aromatic rings of the calixarene molecules (Figure 5). In this porous open structure, these channels correspond to 16.9% of the total crystal volume. The mean diameter of each channel is about 6.6 Å with a minimum diameter of 4.0 Å. These parallel nanochannels are arranged in a distorted honeycomb motif with about 12−14 Å between the centers of the channels (Figure S12). The interchannel space, which does not contain solvent molecules, is to some extent filled by the lipophilic lower rim propyl chains arranged in various conformations with partial occupancy.

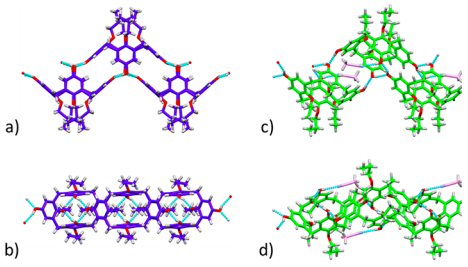

Figure 4. Side and top views of the two distinct linear polymeric chain assemblies of **3** found in SOF-2 propagated by H-bonding interactions. (a, b) Supramolecular chain formed by the C_2 symmetric calixarene in blue. (c, d) Second type of polymeric chain in green, with insertion of acetonitrile molecules in pink which breaks the 2-fold symmetry.

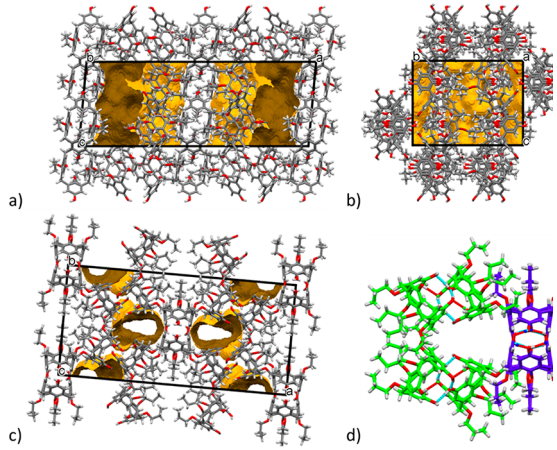

Figure 5. Supramolecular structure of SOF-2. Orthogonal representation of the crystal packing (a−c) following the convention used in the International Tables of Crystallography. Stick models of **3** in CPK colors and contact surface contours defining the nanochannels in the unit cell are shown. (d) Nanochannels formed by the two types of polymeric chains of **3** (blue and green) viewed along the c axis.

When tetrol **3** is crystallized in the presence of hygroscopic NaI in $CHCl_3/CH_3CN$ solvent, it gives rise to solid-state assembly SOF-3, which is quite different with respect to both SOF-1 and SOF-2. The asymmetric unit of the monoclinic ($P2_1/c$) crystal is composed of one tetrol **3** molecule complexing a sodium ion at the lower rim, one CH_3CN guest solvent molecule, one iodide counterion, and two cocrystallized water molecules (Figure S13). In this case, the basic structural element is determined by a Na^+@**3** complex where the sodium cation is symmetrically bound to the four ethereal O atoms at the lower rim (Figure 2c).[46−48] Its coordination sphere is completed by an additional H_2O molecule interacting from the bottom, which is H-bonded to the iodide anion and to a CH_3CN molecule hosted in the cup of another calixarene molecule. The sodium coordination provokes the opening of the calixarene cup (Figure 2d). All four phenyl rings are outwardly inclined with dihedral angles ranging from 110 to 117° with respect to the methylene plane. This preorganized molecular conformation of **3**, which

https://doi.org/10.1021/acs.cgd.1c00828
Cryst. Growth Des. 2021, 21, 6357−6363

approaches to a 4-fold symmetry, permits a CH_3CN molecule to be hosted inside the cavity through a characteristic $CH_3-\pi$ interaction (Figure 2c). The above-mentioned H-bond interactions between the sodium-coordinated water molecules and the acetonitrile guests produce a column of isooriented host–guest complexes parallel to the *c* axis. The iodide anions bridge these columns by H-bonding two OH groups of calixarene molecules related by translation along the *b* axis. This gives rise to a 2D H-bond network on the *ac* plane (Figure 6a). The OH groups of **3** also mutually interact to give

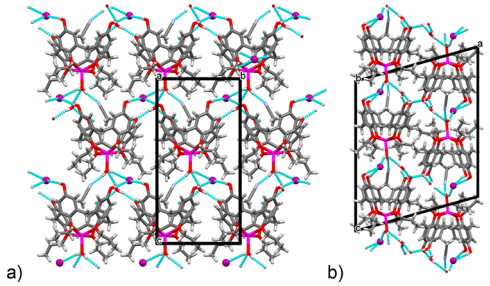

Figure 6. Supramolecular structure of SOF-3. (a) One layer of the 2D H-bond network involving the water molecules coordinated to the sodium ions (magenta), the acetonitrile guests, and the iodide anions (violet spheres). (b) The OH groups of **3** mutually interact to give H-bonded double layers antiparallel with respect to the calixarene cups.

H-bonded double layers that are antiparallel with respect to the calixarene cups (Figure 6b). The overall effect is a relatively compact crystal packing without the presence of solvent channels. Therefore, the coordination of the sodium ions produces a more preorganized and rigid calixarene cup available for the coordination of a suitable guest.

On the other hand, by opening the pinched conformation with facing phenol rings, the calixarene loses the ability to form complementary strong H-bond interactions responsible for formation of crystal nanochannels, as in SOF-1 and SOF-2.

At this point is also of interest to consider the assembling properties of dibromo-calix[4]arene-diol **5**, in comparison to tetrol **3**. Crystallization of **5** from CH_3OH gives rise to solid state assembly SOF-4. The asymmetric unit of the monoclinic ($P2_1/n$) crystal is composed of 2 molecules of **5** and 1.2 cocrystallized water molecules (Figure S14). The calixarene cone conformation is pinched at the phenol groups. The bromo-phenyl rings are outward oriented and form dihedral angles with the methylene plane in the 143–147° range, while the phenolic rings are inward oriented with dihedral angles between 72 and 84°. Therefore, the pinched cone conformation of calixarene is similar to that observed in SOF-1 and SOF-2 (Figure 2e,f). However, the presence of two bromine atoms in place of two hydroxyl groups, which can be involved only as a weak H-bond acceptor, dramatically affects the possibility to form the mutual intermolecular H-bond network responsible for the open structures observed in SOF-1 and SOF-2. In fact, in SOF-4, the H-bond network is limited to four molecules of **5** and four water molecules in partially occupied sites (Figure 7). The overall result is a compact packed structure, without channels and molecular cavities (Figure S15).

CONCLUSIONS

In the present investigation, we have studied the formation of SOFs using the cone-shaped calix[4]arene-tetrol **3**. This

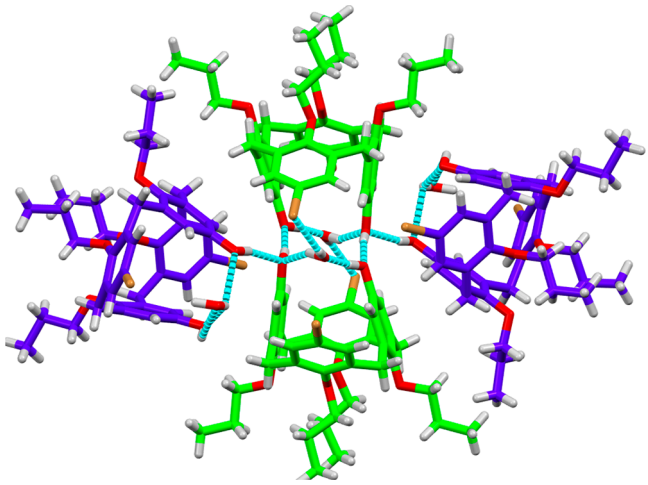

Figure 7. Supramolecular structure of SOF-4. The H-bond network is limited to four molecules of **5** and four water molecules. The tetrameric assembly lies on an inversion center and is composed of two crystallographic independent molecules (blue and green) and two inversion generated molecules.

molecule has the ability to form open structures due to the presence of four OH groups at the upper rim, which allows the construction of a H-bonded framework. Using different crystallization solvents, two different types of SOFs containing parallel nanochannels were formed, with similar void volume (16–17%). Very significant differences were observed in the nature of the channel walls, in the dimension of the channels, and in the pattern of the parallel channels. In the presence of water, hydrophilic channels are formed by the phenolic OH groups which point toward the center of the SOF-1 channels. The mean diameter of each channel is about 8.5 Å, with a minimum diameter of 5.2 Å, and they are organized in a 17.2 × 20.1 $Å^2$ rectangular pattern. In the presence of acetonitrile, channels delimited by aromatic walls are formed. With respect to SOF-1, the channels of SOF-2 are smaller, with a mean/minimum diameter of 6.6/4.0 Å, but are more densely arranged in a distorted honeycomb motif with sides of 12–14 Å. Both SOFs are characterized by a pinched cone conformation of **3** which closes the calixarene cup, even in the presence of potential guest molecules, such as the acetonitrile. In order to force the opening of this pinched cone conformation, we introduced a sodium ion, which coordinates **3** at the lower rim. In fact, in the solid state, the metal ion coordination of the OPr groups produces a more open, rigid, and symmetric cone conformation. This Na^+@**3** adduct was then able to host the acetonitrile guest molecule in the molecular cavity of calix[4]arene cup. However, the geometric reorganization of the phenolic groups of Na^+@**3** produces SOF-3, a more compact structure without channels. Similarly, dibromo-calix[4]arene-diol **5** also forms compact structure SOF-4 despite the fact that it exhibits the pinched cone conformation of **3**. Therefore, the present investigation indicates that the nature and architecture of open structures based on a calix[4]arene-tetrol (SOF-1 and SOF-2) are determined by the presence of a pinched cone conformation with four OH groups, which can be influenced by the solvent.

https://doi.org/10.1021/acs.cgd.1c00828
Cryst. Growth Des. 2021, 21, 6357–6363

■ ASSOCIATED CONTENT

Supporting Information

The Supporting Information is available free of charge at https://pubs.acs.org/doi/10.1021/acs.cgd.1c00828.

^{1}H and ^{13}C NMR, HR-MS, detail of X-ray data collection, processing, and refinement statistics, thermal treatment (PDF)

Accession Codes

CCDC 2094512−2094515 contain the supplementary crystallographic data for this paper. These data can be obtained free of charge via www.ccdc.cam.ac.uk/data_request/cif, or by emailing data_request@ccdc.cam.ac.uk, or by contacting The Cambridge Crystallographic Data Centre, 12 Union Road, Cambridge CB2 1EZ, UK; fax: +44 1223 336033.

■ AUTHOR INFORMATION

Corresponding Authors

Placido Neri − *Dipartimento di Chimica e Biologia "A. Zambelli", Università di Salerno, I-84084 Fisciano, Salerno, Italy*; Email: neri@unisa.it

Silvano Geremia − *Centro di Eccellenza in Biocristallografia, Dipartimento di Scienze Chimiche e Farmaceutiche, Università di Trieste, I-34127 Trieste, Italy*; orcid.org/0000-0002-0711-5113; Email: sgeremia@units.it

Authors

Neal Hickey − *Centro di Eccellenza in Biocristallografia, Dipartimento di Scienze Chimiche e Farmaceutiche, Università di Trieste, I-34127 Trieste, Italy*; orcid.org/0000-0003-1271-5719

Veronica Iuliano − *Dipartimento di Chimica e Biologia "A. Zambelli", Università di Salerno, I-84084 Fisciano, Salerno, Italy*; orcid.org/0000-0001-9787-5441

Carmen Talotta − *Dipartimento di Chimica e Biologia "A. Zambelli", Università di Salerno, I-84084 Fisciano, Salerno, Italy*; orcid.org/0000-0002-2142-6305

Margherita De Rosa − *Dipartimento di Chimica e Biologia "A. Zambelli", Università di Salerno, I-84084 Fisciano, Salerno, Italy*; orcid.org/0000-0001-7451-5523

Annunziata Soriente − *Dipartimento di Chimica e Biologia "A. Zambelli", Università di Salerno, I-84084 Fisciano, Salerno, Italy*; orcid.org/0000-0001-6937-8405

Carmine Gaeta − *Dipartimento di Chimica e Biologia "A. Zambelli", Università di Salerno, I-84084 Fisciano, Salerno, Italy*; orcid.org/0000-0002-2160-8977

Complete contact information is available at: https://pubs.acs.org/10.1021/acs.cgd.1c00828

Author Contributions

The manuscript was written through contributions of all authors. All authors have given approval to the final version of the manuscript.

Funding

The authors acknowledge for financial support MIUR through the PRIN project 20179BJNA2.

Notes

The authors declare no competing financial interest.

■ ACKNOWLEDGMENTS

We thank the Elettra Synchrotron (Trieste, Italy) and the staff of the XRD1 beamline for their technical assistance.

■ ABBREVIATIONS

SOF, supramolecular organic framework; MOF, metal−organic framework; COF, covalent organic framework; M-SOF, macrocycle-based SOF

■ REFERENCES

(1) Sozzani, P.; Bracco, S.; Comotti, A.; Ferretti, L.; Simonutti, R. Methane and carbon dioxide storage in a porous van der Waals crystal. *Angew. Chem., Int. Ed.* **2005**, *44*, 1816−1820.

(2) He, Y.; Xiang, S.; Chen, B. A microporous hydrogen-bonded organic framework for highly selective C_2H_2/C_2H_4 separation at ambient temperature. *J. Am. Chem. Soc.* **2011**, *133*, 14570−14573.

(3) Mastalerz, M.; Oppel, I. M. Rational construction of an extrinsic porous molecular crystal with an extraordinary high specific surface area. *Angew. Chem., Int. Ed.* **2012**, *51*, 5252−5255.

(4) Luo, X.-Z.; Jia, X.-J.; Deng, J.-H.; Zhong, D.-C.; Liu, H.-J.; Wang, K.-J.; Zhong, D.-C. A microporous hydrogen-bonded organic framework: exceptional stability and highly selective adsorption of gas and liquid. *J. Am. Chem. Soc.* **2013**, *135*, 11684−11687.

(5) Li, P.; He, Y.; Guang, J.; Weng, L.; Zhao, J. C.-G.; Xiang, S.; Chen, B. A homochiral microporous hydrogen-bonded organic framework for highly enantioselective separation of secondary alcohols. *J. Am. Chem. Soc.* **2014**, *136*, 547−549.

(6) Yamamoto, A.; Hamada, T.; Hisaki, I.; Miyata, M.; Tohnai, N. Dynamically deformable cube-like hydrogen-bonding networks in water-responsive diamondoid porous organic salts. *Angew. Chem., Int. Ed.* **2013**, *52*, 1709−1712.

(7) Li, P.; He, Y.; Zhao, Y.; Weng, L.; Wang, H.; Krishna, R.; Wu, H.; Zhou, W.; O'Keeffe, M.; Han, Y.; Chen, B. A rod-packing microporous hydrogen-bonded organic framework for highly selective separation of C_2H_2/CO_2 at room temperature. *Angew. Chem., Int. Ed.* **2014**, *54*, 574−577.

(8) Wang, H.; Li, B.; Wu, H.; Hu, T.-L.; Yao, Z.; Zhou, W.; Xiang, S.; Chen, B. A flexible microporous hydrogen-bonded organic framework for gas sorption and separation. *J. Am. Chem. Soc.* **2015**, *137*, 9963−9970.

(9) Yang, W.; Greenaway, A.; Lin, X.; Matsuda, R.; Blake, A. J.; Wilson, C.; Lewis, W.; Hubberstey, P.; Kitagawa, S.; Champness, N. R.; Schröder, M. Exceptional thermal stability in a supramolecular organic framework: porosity and gas storage. *J. Am. Chem. Soc.* **2010**, *132*, 14457.

(10) Lü, J.; Perez-Krap, C.; Suyetin, M.; Alsmail, N. H.; Yan, Y.; Yang, S.; Lewis, W.; Bichoutskaia, E.; Tang, C. C.; Blake, A. J.; Cao, R.; Schröder, M. A robust binary supramolecular organic framework (SOF) with high CO_2 adsorption and selectivity. *J. Am. Chem. Soc.* **2014**, *136*, 12828−12831.

(11) Sumida, K.; Rogow, D. L.; Mason, J. A.; McDonald, T. M.; Bloch, E. D.; Herm, Z. R.; Bae, T.-H.; Long, J. R. Carbon dioxide capture in metal-organic frameworks. *Chem. Rev.* **2012**, *112*, 724−781.

(12) Yang, S.; Lin, X.; Lewis, W.; Suyetin, M.; Bichoutskaia, E.; Parker, J.; Tang, C. C.; Allan, D. R.; Rizkallah, P. J.; Hubberstey, P.; Champness, N. R.; Thomas, K. M.; Blake, A. J.; Schröder, M. A partially interpenetrated metal-organic framework for selective hysteretic sorption of carbon dioxide. *Nat. Mater.* **2012**, *11*, 710−716.

(13) Yang, S.; Sun, J.; Ramirez-Cuesta, A. J.; Callear, S. K.; David, W. I. F.; Anderson, D.; Newby, R.; Blake, A. J.; Parker, J. E.; Tang, C. C.; Schröder, M. Selectivity and direct visualization of carbon dioxide and sulfur dioxide in a decorated porous host. *Nat. Chem.* **2012**, *4*, 887−849.

(14) Zhu, X.-D.; Zhang, K.; Wang, Y.; Long, W.-W.; Sa, R.-J.; Liu, T.-F.; Lü, J. Fluorescent metal organic framework (MOF) as a highly sensitive and quickly responsive chemical sensor for the detection of antibiotics in simulated wastewater. *Inorg. Chem.* **2018**, *57*, 1060−1065.

(15) Chandra, S.; Kundu, T.; Kandambeth, S.; BabaRao, R.; Marathe, Y.; Kunjir, S. M.; Banerjee, R. Phosphoric acid loaded azo (-N = N-) based covalent organic framework for proton conduction. *J. Am. Chem. Soc.* **2014**, *136*, 6570−6573.

(16) Spitler, E. L.; Koo, B. T.; Novotney, J. L.; Colson, J. W.; Uribe-Romo, F. J.; Gutierrez, G. D.; Clancy, P.; Dichtel, W. R. A 2D covalent organic framework with 4.7-nm pores and insight into its interlayer stacking. *J. Am. Chem. Soc.* **2011**, *133*, 19416−19421.
(17) Kim, H.; Kim, Y.; Yoon, M.; Lim, S.; Park, S. M.; Seo, G.; Kim, K. Highly selective carbon dioxide sorption in an organic molecular porous material. *J. Am. Chem. Soc.* **2010**, *132*, 12200−12202.
(18) Tian, J.; Ma, S.; Thallapally, P. K.; Fowler, D.; McGrail, B. P.; Atwood, J. L. Cucurbit[7]uril: an amorphous molecular material for highly selective carbon dioxide uptake. *Chem. Commun.* **2011**, *47*, 7626−7628.
(19) Zhang, K.-D.; Tian, J.; Hanifi, D.; Zhang, Y.; Sue, A. C.-H.; Zhou, T.-Y.; Zhang, L.; Zhao, X.; Liu, U.; Li, Z.-T. Toward a singlelayer two-dimensional honeycomb supramolecular organic framework in water. *J. Am. Chem. Soc.* **2013**, *135*, 17913−17918.
(20) Hisaki, I.; Nakagawa, S.; Ikenaka, N.; Imamura, Y.; Katouda, M.; Tashiro, M.; Tsuchida, H.; Ogoshi, T.; Sato, H.; Tohnai, N.; Miyata, M. A series of layered assemblies of hydrogen-bonded, hexagonal networks of C3-symmetric π-conjugated molecules: A potential motif of porous organic materials. *J. Am. Chem. Soc.* **2016**, *138*, 6617−6628.
(21) Martí-Rujas, J.; Colombo, L.; Lü, J.; Dey, A.; Terraneo, G.; Metrangolo, P.; Pilati, T.; Resnati, G. Hydrogen and halogen bonding drive the orthogonal self-assembly of an organic framework possessing 2D channels. *Chem. Commun.* **2012**, *48*, 8207−8209.
(22) Bhogala, B. R.; Basavoju, S.; Nangia, A. Three-component carboxylic acid-bipyridine lattice inclusion host. Supramolecular synthesis of ternary cocrystals. *Cryst. Growth Des.* **2005**, *5*, 1683−1686.
(23) Patil, R. S.; Banerjee, D.; Zhang, C.; Thallapally, P. K.; Atwood, J. L. Selective CO_2 Adsorption in a supramolecular organic framework. *Angew. Chem., Int. Ed.* **2016**, *55*, 4523−4526.
(24) Dewal, M. B.; Lufaso, M. W.; Hughes, A. D.; Samuel, S. A.; Pellechia, P.; Shimizu, L. S. Absorption properties of a porous organic crystalline apohost formed by a self-assembled bis-urea macrocycle. *Chem. Mater.* **2006**, *18*, 4855−4864.
(25) Lim, S.; Kim, H.; Selvapalam, N.; Kim, K. J.; Cho, S. J.; Seo, G.; Kim, K. Cucurbit[6]uril: Organic molecular porous material with permanent porosity, exceptional stability, and acetylene sorption properties. *Angew. Chem., Int. Ed.* **2008**, *47*, 3352−3355.
(26) Ogoshi, T.; Sueto, R.; Yoshikoshi, K.; Yamagishi, T. One-dimensional channels constructed from per-hydroxylated pillar[6]-arene molecules for gas and vapour adsorption. *Chem. Commun.* **2014**, *50*, 15209−15211.
(27) Tan, L. L.; Zhu, Y. L.; Long, H.; Jin, Y. H.; Zhang, W.; Yang, Y. W. Pillar[n]arene-based supramolecular organic frameworks with high hydrocarbon storage and selectivity. *Chem. Commun.* **2017**, *53*, 6409−6412.
(28) Jie, K.; Liu, M.; Zhou, Y.; Little, M. A.; Pulido, A.; Chong, S. Y.; Stephenson, A.; Hughes, A. R.; Sakakibara, F.; Ogoshi, T.; Blanc, F.; Day, G. M.; Huang, F.; Cooper, A. I. Near-ideal xylene selectivity in adaptive molecular pillar[n]arene crystals. *J. Am. Chem. Soc.* **2018**, *140*, 6921−6930.
(29) Patil, R. S.; Zhang, C.; Barnes, C. L.; Atwood, J. L. Construction of supramolecular organic frameworks based on noria and bipyridine type spacers. *Cryst. Growth Des.* **2017**, *17*, 7−10.
(30) (a) Dalgarno, S. J.; Thallapally, P. K.; Barbour, L. J.; Atwood, J. L. Engineering void space in organic van der Waals crystals: calixarenes lead the way. *Chem. Soc. Rev.* **2007**, *36*, 236−245. (b) Patil, R. S.; Drachik, A. M.; Kumari, H.; Barnes, C. L.; Deakyne, C. A.; Atwood, J. L. Solvent induced manipulation of supramolecular organic frameworks. *Cryst. Growth Des.* **2015**, *15*, 2781−2786. (c) Patil, R. S.; Kumari, H.; Barnes, C. L.; Atwood, J. L. Anion- and spacer-directed host-guest complexes of bipyridine with pyrogallol[4]arene. *Chem. - Eur. J.* **2015**, *21*, 10431−10435. (d) Patil, R. S.; Kumari, H.; Barnes, C. L.; Atwood, J. L. Engineering supramolecular organic frameworks (SOFs) of C-alkylpyrogallol[4]-arene with bipyridine-based spacers. *Chem. Commun.* **2015**, *51*, 2304−2307.
(31) Hong, B. H.; Lee, J. Y.; Lee, C.-W.; Kim, J. C.; Bae, S. C.; Kim, K. S. Self-assembled arrays of organic nanotubes with infinitely long one-dimensional H-bond chains. *J. Am. Chem. Soc.* **2001**, *123*, 10748−10749.
(32) Suh, S. B.; Kim, J. C.; Choi, Y. C.; Yun, S.; Kim, K. S. Nature of one-dimensional short hydrogen bonding: Bond distances, bond energies, and solvent effects. *J. Am. Chem. Soc.* **2004**, *126*, 2186−2193.
(33) Hong, B. H.; Bae, S. C.; Lee, C.-W.; Jeong, S.; Kim, K. S. Ultrathin single-crystalline silver nanowire arrays formed in an ambient solution phase. *Science* **2001**, *294*, 348−351.
(34) Tedesco, C.; Immediata, I.; Gregoli, L.; Vitagliano, L.; Immirzi, A.; Neri, P. Interconnected water channels and isolated hydrophobic cavities in a calixarene-based, nanoporoussupramolecular architecture. *CrystEngComm* **2005**, *7*, 449−453.
(35) Thallapally, P. K.; McGrail, B. P.; Atwood, J. L.; Gaeta, C.; Tedesco, C.; Neri, P. Carbon dioxide capture in a self-assembled organic nanochannels. *Chem. Mater.* **2007**, *19*, 3355−3357.
(36) Tedesco, C.; Erra, L.; Brunelli, M.; Cipolletti, V.; Gaeta, C.; Fitch, A. N.; Atwood, J. L.; Neri, P. Methane adsorption in a supramolecular organic zeolite. *Chem. - Eur. J.* **2010**, *16*, 2371−2374.
(37) Tedesco, C.; Erra, L.; Immediata, I.; Gaeta, C.; Brunelli, M.; Merlini, M.; Meneghini, C.; Pattison, P.; Neri, P. Solvent induced pseudopolymorphism in a calixarene-based porous host framework. *Cryst. Growth Des.* **2010**, *10*, 1527−1533.
(38) Erra, L.; Tedesco, C.; Immediata, I.; Gregoli, L.; Gaeta, C.; Merlini, M.; Meneghini, C.; Brunelli, M.; Fitch, A. N.; Neri, P. Inclusion properties of volatile organic compounds in a calixarene-based organic zeolite. *Langmuir* **2012**, *28*, 8511−8517.
(39) Arduini, A.; Mirone, L.; Paganuzzi, D.; Pinalli, A.; Pochini, A.; Secchi, A.; Ungaro, R. New calix[4]arenes having electron donating groups at the upper rim as molecular platforms and host molecules. *Tetrahedron* **1996**, *52*, 6011−6018.
(40) Fulmer, G. R.; Miller, A. J. M.; Sherden, N. H.; Gottlieb, H. E.; Nudelman, A.; Stoltz, B. M.; Bercaw, J. E.; Goldberg, K. I. NMR chemical shifts of trace impurities: Common laboratory solvents, organics, and gases in deuterated solvents relevant to the organo-metallic chemist. *Organometallics* **2010**, *29*, 2176−2179.
(41) Pellet-Rostaing, S.; Chitry, F.; Nicod, L.; Lemaire, M. Synthesis and complexation properties of 1,3-alternate calix[4]arene-bis(crown-6) derivatives. *J. Chem. Soc., Perkin Trans. 2* **2001**, *8*, 1426−1432.
(42) Zyryanov, G. V.; Kang, Y.; Rudkevich, D. M. Sensing and fixation of NO_2/N_2O_4 by calix[4]arenes. *J. Am. Chem. Soc.* **2003**, *125*, 2997−3007.
(43) Billo, F.; Musau, R. M.; Whiting, A. Approaches to polymetallatedcalixarene derivatives. *ARKIVOC* **2006**, *2006*, 199−210.
(44) Gutsche, C. D.; Pagoria, P. F. Calixarenes. 16. Functionalized calixarenes: the direct substitution route. *J. Org. Chem.* **1985**, *50*, 5795−5802.
(45) Giuliani, M.; Morbioli, I.; Sansone, F.; Casnati, A. Mouldingcalixarenes for biomacromolecule targeting. *Chem. Commun.* **2015**, *51*, 14140−14159.
(46) Blixt, J.; Detellier, C. Kinetics and mechanism of the sodium cation complexation by 5,11,17,23-tetra-p-tert-butyl-25,26,27,28-tetramethoxycalix[4]arene in solution. *J. Am. Chem. Soc.* **1995**, *117*, 8536−8540.
(47) Blixt, J.; Detellier, C. Conformational dynamics of calixarenes; kinetics of conformationalinterconversion in5,11,17,23-tetra-p-tert-butyl-25,26,27,28-tetramethoxycalix[4]-arene under entropic control. *J. Am. Chem. Soc.* **1994**, *116*, 11957−11960.
(48) Debbert, S. L.; Hoh, B. D.; Dulak, D. J. Synthesis and characterization of calixarenetetraethers: An exercise in supra-molecular chemistry for the undergraduate organic laboratory. *J. Chem. Educ.* **2016**, *93*, 372−375.

https://doi.org/10.1021/acs.cgd.1c00828
Cryst. Growth Des. 2021, 21, 6357−6363